의학박사 학위논문

Pretreatment with Low-dose Fimasartan, One of Angiotensin Receptor Blockers, Inhibits NLRP3 Inflammasome Activation in a Rat Intracerebral Hemorrhage Model

백서 뇌출혈 모델에서 저농도 피마사탄 전처치 후 NLRP3 인플라마좀 활성화 억제를 통한 뇌손상 보호 효과에 대한 연구

2017 년 02 월

서울대학교 대학원

의학과 중개의학 전공

양 슈 리

Pretreatment with Low-dose Fimasartan Inhibits NLRP3 Inflammasome Activation in a Rat Intracerebral Hemorrhage Model

백서 뇌출혈 모델에서 저농도 피마사탄 전처치 후 NLRP3 인플라마좀 활성화 억제를 통한 뇌손상 보호 효과에 대한 연구

지도교수 윤병우

이 논문을 의학박사 학위논문으로 제출함

2016 년 10 월

서울대학교 대학원

의학과 중개의학 전공

양 슈 리

양슈리의 박사학위논문을 인준함

2016 년 12 월

위원장	손철호	(인)
부위원장	윤병우	(인)
위원	김만호	(인)
위원	권형민	(인)
위원	박종무	(인)

학위논문 원문 이용에 대한 동의서

본인은 아래의 학위논문이 제3자의 권리를 침해하지 않았음을 서약하며, 서울대학교가 다음과 같이 저작물을 이용하는 것에 동의합니다.

논문 제목	**백서 뇌출혈 모델에서 저농도 피마사탄 전처치 후 NLRP3 인플라마좀 활성화 억제를 통한 뇌손상 보호 효과에 대한 연구**
학위 구분	**석사 □/ 박사 □**
학 과	의학과
학 번	2014-31395
연 락 처	010-9251-1891

1. 본인은 서울대학교가 위 저작물을 인터넷 등 정보통신망을 통해 복제·전송·배포하는 것에 동의합니다.

2. 본인은 서울대학교가 위 저작물에 대해 무료로 온라인 서비스를 제공하는 것에 동의합니다.

3. 서울대학교는 내용을 변경하지 않는 범위 안에서 위 저작물을 다른 파일 형식으로 변경할 수 있습니다.

4. 본인은 위 저작물의 저작권을 타인에게 양도하거나 출판을 허락하는 등 동의 내용을 변경하고자 할 경우 소속대학(원)에 공개의 유보 또는 해지를 즉시 통보하겠습니다.

5. 서울대학교는 저작권법 및 도서관법을 준수하며 해당 저작물로 인하여 발생하는 타인에 의한 권리 침해에 대하여 일체의 법적 책임을 지지 않습니다.

제 출 일: 2017 년 02월 01일

저 작 자: 양슈리(인)

서울대학교총장 귀하

ABSTRACT

Pretreatment with Low-dose Fimasartan Inhibits NLRP3 Inflammasome Activation in a Rat Intracerebral Hemorrhage Model

Xiu-Li Yang

Department of Translational Medicine, College of Medicine

The Graduate School

Seoul National University

Background and Purpose: The NLRP3 inflammasome, which is composed of NLRP3 (NOD-Like Receptor family Pyrin domain containing 3), the adaptor molecule apoptosis-associated speck-like protein containing a CARD (ASC) domain and procaspase-1, plays an important role in the immune pathophysiology of secondary damage induced by intracerebral hemorrhage (ICH). This study aims to investigate whether pretreatment with low-dose fimasartan, an angiotension II receptor blocker (ARB), has anti-neuroinflammatory effect in normotensive rats following ICH by inhibiting the activation of the NLRP3 inflammasome.

Materials and Methods: Sprague-Dawley rats were divided into the four groups as follows: sham, vehicle, low-dose (0.5 mg/kg) and regular dose (1.0 and 3.0 mg/kg) fimasartan. These rats were treated

for 30 days before the induction of collagenase-induced ICH and for 2 days after surgery. Brain water content, hematoma volume, neurological functional recovery and blood pressure (BP) were evaluated according to the different doses of fimasartan. The expression of protein, mRNA, pro-inflammatory cytokines and double immunofluorescent staining of the NLRP3 inflammasome components were measured on 1 day post-ICH in the rats administrated with the low-dose fimasartan.

In vitro experiments, we stimulated astrocytes with hemolysate to induce hemorrhagic inflammation. Astrocytes were pretreated with fimasartan at different concentrations and then incubated with hemolysate. Inflammatory cell signaling pathways were assessed by western blotting. Pro-inflammatory mediators were evaluated by real time RT-PCR and ELISA.

Results: ICH rat model resulted in a large hematoma and edema accompanied by the up-regulation of NLRP3/ASC/Caspase-1 and the NF-κB signaling pathway, which subsequently contribute to the release of pro-inflammatory cytokines within one day. Long-term pretreatment with either dose of fimasartan attenuated the ICH-induced edema and improved neurological functional outcomes. BP was regulated by fimasartan in a dose-dependent manner, but with no change in the low-dose. Furthermore, the activation of the NLRP3 inflammasome components and the NF-κB pathway were markedly reduced by low-dose fimasartan. The double immunofluorescent staining of brain cells showed a progressive decrease in co-localization of NLRP3/ASC/Caspase-1 with Iba1 (microglia marker) and GFAP (astrocyte marker) positive cells.

In vitro, the stimulation by hemolysate generated a robust activation of inflammatory response in astrocytes. Pretreatment with fimasartan significantly decreased hemolysate-induced NFκB-related inflammatory pathways induced by hemolysate. This reduction of inflammatory upstream pathways decreased the expression of end-products, COX-2 and interleukin-1.

Conclusions: Our study suggests that the direct anti-inflammatory effect of fimasartan reduces acute ICH-induced damage. Specially, low-dose fimasartan improves the neurological recovery and reduce the edema by inhibiting the NLRP3 inflammasome without affecting BP. Pretreatment with fimasartan

also inhibits hemolysate-induced inflammatory in astrocytes. Of translational significance, fimasartan could potentially target the inflammasome to attenuate secondary injury after ICH.

Keywords: ARBs, Intracerebral hemorrhage, NLRP3 inflammasome, NF-κB, Astrocytes, hemolysate

Student number: 2014-31395

CONTENTS

LIST OF FIGURES

LIST OF TABLES

LIST OF ABBREVIATIONS

ICH: intracerebral hemorrhage

CNS: central nervous system

NLRP3: nucleotide binding and oligomerization domain-like receptor family pyrin domain-containing 3

ASC: apoptosis-associated speck-like protein containing a caspase recruitment domain

IL: interleukin

TNFα: tumor necrosis factor α

NF-κB: nuclear factor kappa-light-chain-enhancer of activated B cells

mNSS: modified Neurological Severity Score

IF: Immunofluorescence Staining

PCR: polymerase chain reaction

ELISA: enzyme linked immunosorbent assay

Iba1: ionized calcium binding adaptor molecule 1

GFAP: Glial fibrillary acidic protein

Fima: fimasartan

Hemo: hemolysate

INTRODUCTION

Intracerebral hemorrhage (ICH) is one of the subtypes of stroke that is characterized by high mortality and morbidity, and represents approximately 10-15% of stroke worldwide each year (1). Although the number of hospital admissions for ICH has increased in the past ten years, the mortality rate has not decreased due to the increasing number of the elderly affected by ICH, the racial differences in the incidence of ICH and the increased use of anticoagulants (2, 3). Currently, there are no effective therapies for ICH because of the complex and poorly understood etiology. Therefore, a better understanding the pathophysiology of injury after ICH has important implications for patients.

Hemolysate, as one of the products of hemoglobin breakdown, can be transported into any cell within contact. It is a spasminogen in SAH and contributes to the formation of brain edemas after ICH (4). The toxicity of hemolysate and hemoglobin leads to inflammation and apoptosis of brain cells after ICH (5-7). Previous studies have established hemolysate stimulating brain cells as well characterized model of hemorrhagic research (8, 9).

Accumulating evidence suggests that inflammatory factors are involved in the secondary brain damage induced by ICH; however, the molecular mechanisms underlying the innate immune response in ICH are not fully understood (10, 11). Recently, the so-called inflammasome have been found to play a key role in innate immune response in the central nervous system (CNS) diseases (12-15). The inflammasome regulates diverse inflammatory response and exists in all organs, including the brain (16). Typically, the inflammasome is composed of at least one member of the cytosolic innate immune sensor family, the NOD-like receptors (NLRs), coupled with the adaptor apoptosis-associated speck like protein containing a caspase recruitment domain (ASC or PYCARD) and caspase-1 (17). The NLRP3 inflammasome is the best characterized to date and is activated by several endogenous and exogenous signals, including PAMPs, DAMPs and bacterial toxins (18-20). Activation of the NLRP3 inflammasome activates caspase-1 and induces the secretion of mature cytokines, such as IL-1β. The processing of cytokine is mediated by two distinct signals. The first signal is the priming signal, which

involves activation of the signaling NF-κB pathway, and the second signal involves the formation of NLRP3 inflammasome complex with cleaved caspase-1 (21). An increasing number of studies have suggested that the NLRP3 inflammasome contributes to brain inflammation in stroke, especially in ICH (22, 23).

In the CNS, angiotensinogen mainly produced by astrocytes and angiotensin II receptors are abundantly presented in the brain (24). Angiotension II receptor antagonists (ARBs) are one of the most effective therapies for hypertension, diabetes and stroke because of their potent anti-inflammatory effects (25). As is well known, As is well known, some ARBs display neuroprotective effects not only in hypertensive but also in normotensive animals with the ability to penetrate the blood-brain barrier (BBB). Preclinical and clinical studies have suggested that most ARBs have the ability to penetrate into the brain, especially with chronic treatment or some pathologic conditions that make the BBB more permissive. In particular, pretreatment with low-dose ARBs, such as telmisartan and candesartan, have neuroprotective effects without affecting blood pressure (BP) in normotensive rodents (26, 27). Furthe rmore, a recent retrospective study found that prestroke ARB treatment might reduce the mortality of ischemic stroke patients (29). Fimasartan (BR-A-657) is a novel, non-peptide ARB, which was approved by the Korean Food and Drug Administration KFDA in 2010 (28). Fimasartan, which was rapidly absorbed and well tolerated, can effectively regulate BP in a dose dependent manner. Our previous study found that fimasartan has anti-inflammatory effects in vivo of a model of ischemic stroke and in vitro on astrocytes (30, 31).

Therefore, this study aims to investigate the mechanism of low-dose fimasartan in the attenuation of neuroinflammatory response in acute ICH stroke beyond its ability to control BP. After long-term pretreatment with different doses of fimasartan to normotensive rats, we first evaluated its ability to regulate BP after ICH, and then, we selected the low-dose fimasartan as the effective therapeutic concentration that does not lower BP. Furthermore, we investigated the role of low-dose fimasartan on the two signals of inflammatory induced by ICH, the NLRP3 inflammasome and the NF-κB pathway.

MATERIALS AND METHODS

In Vivo Experiments

Treatment of Fimasartan

Fimasartan, obtained from Boryung Pharmaceutical Company, was dissolved in phosphate- buffered saline (1 mg/mL) and diluted with sterile water to constitute either the low dose (0.5 mg/kg, p.o.) or regular dose (1.0 and 3.0 mg/kg, p.o.) according to our previous study. Fimasartan or Distilled water (DW) was administrated orally for 30 days prior to the induction of ICH and for 2 days after the surgery.

Induction of Intracerebral Hemorrhage

All animal experimental protocols were approved by the National Institutes of Health Animal Care and Use Committee of the Biomedical Research Institute at Seoul National University Hospital. Four-week-old male Sprague-Dawley rats (Koatech, Seoul, Republic of Korea) weighing 65-75 g were randomized into four groups: sham, ICH + DW, ICH + low-dose fimasartan and ICH +regular dose fimasartan. Sham-operated rats only underwent needle insertion without collagenase injection. The rats in the ICH groups were fixed in a stereotaxic frame (David Kopf Instruments, Tujunga, CA, USA). A 30-gauge Hamilton syringe needle was inserted into the striatum (3.0 mm left lateral to the midline, 0.2 mm posterior to the bregma and 6.0 mm in depth below the skull), and the rats were then injected intrastriatally with collagenase IV (0.6 U in 1 uL saline, Sigma). These animals were assessed by observing the forelimb flexion and contralateral circling to confirm the success of ICH surgery.

Monitoring of Blood Pressure

The noninvasive mean BP levels were monitored during one month of fimasartan administration using a CODA Noninvasive Blood Pressure System (Kent Scientific Corporation, Torrington, CT). The mean BP was recorded using a band attached to the rat's tail (homologated by Bland-Altman testing) (32), which has been recommended by the American Heart Association to monitor the BP levels of experimental animal (33). Noninvasive BP monitoring was performed on days 28, 14, 7, 3 and at baseline during the administration of fimasartan. (n = 10 per group) (Fig.1a).

Measuring the Brain Water Content and Hemorrhage Volume

We analyzed the brain water content and hematoma volume 3 days after surgery because edema is the most severe on the three days after ICH (34). After rats were sacrificed on 72 h after ICH, the brains (n = 12 per group) were divided into two hemispheres along the midline and immediately weighed using an electric analytical balance to obtain the wet weight. The brain samples were then dried in a gravity oven at 100°C for 24 h to obtain the dry weight. Water content = (wet content-dry content) / (wet content) x 100 (35).

To evaluate the hemorrhagic lesion volume, the brains (n = 8 per group) were serially sectioned at 1-mm intervals in the coronal plane through the needle entry site. The sections both anterior and posterior to the needle entry site were obtained. The hematoma area of each section was measured using Image J (National Institutes of Health, Bethesda, MD) from digital photographs of the serial slices. The total hematoma volume (mm^3) was calculated by summing the hematoma area in each section and multiplying by the thickness of the sections (36).

Behavioral Testing

Two behavioral tests, the modified Neurological Severity Score (mNSS) and forelimb placing test, were performed by investigators blinded to the groups. The rats were assessed before and 1 h, 1 day and 3 days after ICH (n = 17 per group). The mNSS test includes a composite of motor (six

points), sensory (two points), and beam balance (six points) tests, in addition to the absence of reflexes and presence of abnormal movements (four points). The mNSS is graded on a scale of 0-18 (normal score = 0; maximal deficit score = 18) to determine impairment (37).

Forelimb placing asymmetry was scored using the vibrissae-elicited forelimb placing test (38). The rats were held by their torsos allowing their forelimbs to hang free. Each forelimb was tested by stimulating their ipsilateral vibrissae on the edge of countertop once per trial for 10 trials. Intact rats stretch each forelimb quickly on the edge of the table in response to vibrissae stimulation. The total scores are determined by the percentage of successful placing responses.

Western Blotting Analysis

The brain tissue samples from the sham, control and low-dose fimasartan group (n = 5 per group) were homogenized in ice-cold RIPA buffer (Biosesang, Seoul, Korea) after sacrificed on 1 day post-ICH. The protein concentration was determined using a Bradford Protein Assay Kit (Bio-Rad, Hercules, CA, USA). Proteins (60 μg) were separated on 8% and 15% sodium SDS-polyacrylamide gel (SDS-PAGE), using electrophoresis gel and then transferred to polyvinylidene difluoride membranes (Millipore). The membranes were blocked with 5% skim milk and incubated with primary antibodies (listed in Table 1) overnight. After blocking the secondary antibodies with horseradish peroxidase-conjugated anti-rabbit IgG (Santa Cruz Biotechnology), the blots were detected using an enhanced chemiluminescence detection system (Thermo Fisher Scientific, Waltham, MA). Image J (National Institute of Health, Bethesda, MD) was used to analyze the density of the signals. The results are representative of at least three independent experiments for every brain sample.

Quantitative Real-Time PCR

The brain tissue was rinsed with cold PBS, and total RNA was isolated from the left striatum of every group (n = 5) using TRIzol ® reagent (Invitrogen, La Jolla, CA, USA). A total of 2ug of RNA was converted

into cDNA using TOPscript RT DryMIX (Enzynomics Inc., Korea) according to the manufacturer's instructions. The Taqman probes for NLRP3 mRNA (Assay ID: Rn04244620_m1) and caspase-1 mRNA (Assay ID: Rn00562725_g1) were purchased from Applied Biosystems (Foster City, CA). The sequence specific primers were as follows: ASC, forward, 5'-GCT CAC AAT GTC TGT GCT TAG AG-3'; reverse, 5'-GCA GTA GCC ACA GCT CCA G-3' and rS6, forward 5'-TGC TCT TGG TGA AGA GTG GA-3'; reverse 5'-CAA GAA TGC CCC TTA CTC AAA-3'.Quantitative polymerase chain reaction (qPCR) was performed using SYBR Premix Ex Taq™ (Takara Bio Inc., Shiga, Japan) on an ABI 7500 Real-Time PCR System (Perkin-Elmer Applied Biosystems, Lincoln, CA, USA). The results are presented as the mean ± standard error of the relative mRNA expression normalized to GAPDH or rS6 using the comparative ΔΔCt method.

Cytokine Measurement

The level of cytokines including interleukin-1 beta (IL-1β) and TNF-α were quantified by single-plex ELISA kit specific for rat tissue (n = 5 per group) according to the manufacturer's instructions (R&D systems). The results are reported based on standards and expressed as pictograms of the measured molecule per mL of serum (pg/mL).

Double Labeled Immunofluorescence Staining and Cell Quantification

Rats (n = 6 per group) were transcardially perfused with saline and 4% paraformaldehyde in 0.1 mol/L (PH 7.4) phosphate-buffered saline at 1 day after ICH. The cryopreserved brain samples were sectioned in the coronal plane at a thickness of 10 μm and mounted onto silane-coated slides (Dako, Glostrup, Denmark). The sections were blocked with 0.5% bovine serum albumin/0.3% Triton x-100 in 10% goat or donkey serum diluted with PBS for 1 h and then incubated with primary antibodies (summarized in Table 1) at 4°C overnight. For double immunofluorescence (IF) staining, specific cellular markers including ionized calcium binding adaptor protein-1 (Iba-1) for microglia

and GFAP (glial fibrillary acidic protein) for astrocytes were used to identify the inflammasome derived from different cell types. The slides were incubated with fluorophore-conjugated secondary antibodies for 1 h at room temperature, and then mounted with DAKO Paramount (DAKO Corporation, Carpinteria, CA) to stain the cell nuclei. The secondary antibodies included goat anti-rabbit IgG labeled with Alexa Fluor 555, goat anti-mouse IgG labeled with Alexa Fluor 488 (Invitrogen; 1:200) or donkey anti-goat IgG labeled with Alexa Fluor 488 (Invitrogen; 1:200). Primary antibody omitted as a negative control for the IF staining. Bright-field and fluorescent micrographs were acquired using a Leica DM5500B microscope (Leica Microsystems) and LAS-AF image acquisition software (Leica Microsystems, Rijswijk, Netherlands).

The number of positive cells in the perihematoma regions was counted in 3 axial sections and at least 4 fields each section per animal through the center of the hemorrhagic lesion by two independent investigators who were masked to the group identification according to established protocols (39). To count the number of positive microglia and astrocytes, 16 high-power fields were obtained from the stained sections through the center of the ICH lesion (Fig.1b) 1 day after ICH. The total counts in the measured sections converted into cell densities for comparison between the ICH groups.

In Vitro Experiments

Astrocyte Cell Culture

Mouse brain astrocytes (Astrocytes Type I clone; ATCC, CRL-2541) were maintained in Dulbecco's modified Eagle's medium (WELGENE Inc., Daegu, Republic of Korea). The medium was changed once daily. Cells were incubated in a humidified incubator maintained at 37°C with an atmosphere of 5% CO_2. Before experiments, astrocytes were starved in 0.2% serum medium for 12 h, and then were incubated in the presence or absence of fimasartan for 12 h before stimulated with or without 10% hemolysate for the durations indicated.

Preparation of Hemolysate

Hemolysate was prepared from fresh rat arterial blood using methods previously described (29). Heparinized rat arterial blood was centrifuged at 2,500 g for 15 min at 4°C, and the supernatant was aspirated. The erythrocyte containing layer was washed three times with cold saline solution, and then lysed by four freeze/thaw cycles. Following a 1:1 dilution with phosphate buffer saline, the erythrocytes debris was centrifuged at 31,000 g for 15 min, and the supernatant was collected and stored at -80°C. The concentration of hemolysate was determined by measuring the spectra of hemoglobin on a spectrophotometer. The detection of absorbance peaks at 540 and 576 nm confirmed the existence of oxyhemoglobin. The concentration of oxyhemoglobin in the 100% hemolysate was 10.92 nm. We used 10% hemolysate by volume of cell media.

Nuclear Protein Extraction

For the analysis of NFκB translocation, astrocyte nuclear protein extracts were prepared using hypotonic lysis buffer A (10 mM HEPEPS, PH7.6, 10 mM KCl, 1 mM DTT, 0.1 mM EDTA, and 0.5 mM phenylmethylsulfonyl fluoride) for 10 min on ice and vortexed for 10 s. The homogenate was spun by centrifugation at 12,000 g for 10 min. The pellet containing nuclear fraction was resuspended in buffer C (20 mM HEPEPS, PH7.6, 1 mM EDTA, 1 mM DTT, 0.5 mM phenylmethylsulfonyl fluoride, 25% glycerol, and 0.4 M NaCl) for 30 min on ice. The supernatant containing nuclear proteins were collected by centrifugation by 13,000 G for 20 min and stored at -80°C. To assay the nuclear protein translocation of NFκB, equal amounts (40 μg) of protein from the nuclear fractions were analyzed by western blot using an anti-NFκB p65 antibody (Abcam, USA), (1:500). The protocol for western blot analysis is descripted below.

Western Blot Analysis

Astrocytes culture medium was discarded and the remaining cells were harvested at the indicated conditions for western blot analysis. The cell pellets were collected by centrifugation, lysed with a protein extraction reagent, and incubated on ice for 30 min. The cell debris was removed by micro-centrifugation. The protein concentration was determined using the Bradford reagent (Bio-Rad, Hercules, CA, USA). Equal amounts of nuclear protein extracts were separated by electrophoresis on an 8−10% sodium SDS-polyacrylamide gel (SDS-PAGE), and then transferred onto polyvinylidene difluoride (PVDF) filters. The filters were incubated overnight in primary antibodies against COX-2 (Abcam, Cambridge, UK), and Anti-β-actin antibody (Sigma-Aldrich, St. Louis, MO, USA) was used as an internal control. After washing with PBS, the membranes were immunoblotted with a secondary horseradish-peroxidase-conjugated antibody. The blots were visualized by enhanced chemiluminescence (Millipore, Bedford, MA).

Quantitative Real-time Polymerase Chain Reaction

For the analysis of mRNA expression by quantitative real-time PCR, astrocytes were harvested after incubation with or without hemolysate in the absence or presence of various different concentrations (10, 30, 100 ng/mL) of fimasartan for 12 h. Total RNA was isolated by using the TRIzol® reagent kit (Invitrogen, La Jolla, CA, USA) following the manufacturer's instructions. For each sample, 1 μg of total RNA was reverse transcribed into cDNA using the RT PreMix kit (AccuPower RT PreMix®, BIONEER). TaqMan probes for COX-2 mRNA (Assay ID: Mm03294838_ g1) and NFκB1 mRNA (Assay ID: Mm00476361_m1) were obtained from Applied Biosystems. Quantitative polymerase chain reaction (qPCR) was performed using TaqMan real-time PCR method on an ABI 7500 Real-Time PCR Systerm (Perkin-Elmer Applied Biosystems, Lincoln, CA, USA). Initial activation of uracil N-glycosylase was performed at 50 °C for 2 min, AmpliTaq Gold was activated at 95 °C for 10 min; the reaction condition for PCR were 45 cycles of denaturation at 95 °C for 15 s, and an annealing extension at 60 °C for 1 min. The threshold cycle (C_T) for each gene was normalized to housekeeping gene GAPDH. The result was calculated according to the ddC_T method of three independent measurements per cDNA.

Enzyme-Linked Immunosorbent Assay (ELISA)

Cells of six groups were seeded at 1.5×10^5 cells/well into 12 well-plates. Astrocytes were pretreated with or without various concentrations (30, 100, 300, 1000 ng/mL) of fimasartan. After 12 h, hemolysate was added and incubated for another 24 h. The supernatant was collected to test the level of interleukin-1 beta (IL-1β) using ELISA kits specific for mouse (R&D systems, Duoset mouse IL-1β) according to the manufacturer's instructions.

Statistical Analysis

The results were expressed as the mean ± SEM. Statistical analysis was performed using Prism (Graphpad Software, La Jolla, CA). We used the Image J (National Institutes of Health, Bethesda, MD) to assess the value. The results from the different groups were analyzed using an unpaired sample *t*-test or repeated measures of analysis of variance followed by Bonferroni's *post hoc* test. To address the differences among all individual groups, we used one-way ANOVA followed by the *post hoc* Newman-Keuls' test and Tukey's multiple comparison analysis test when necessary. The nonparametric Mann-Whitney *U*-test or Wilcoxon signed-rank test was used for unpaired or paired animal samples, respectively. The nonparametric Kruskal-Wallis H test was used to multiple groups. A two-tailed value of $P < 0.05$ was considered significant.

RESULTS

Mean blood pressure levels were regulated by fimasartan in an ICH rat models

To determine whether fimasartan regulate BP in a dose dependent manner, we monitored the mean BP level during the one month of pretreatment with fimasartan. The noninvasive mean BP monitoring showed the change of BP began at 3 days after the start of fimasartan administration. Compared to the control group, the noninvasive mean BP in the low-dose fimasartan group was not significantly different from that of the control group. After treatment with fimasartan for 28 days, the mean BP was 97 ± 2.4 and 97 ± 3.1 mmHg for the control and low-dose fimasartan group, ($p > 0.05$). The regular-dose fimasartan group showed a reduction in the mean BP as early as 3 days into treatment and induced a significant difference starting at 7 days into treatment in a dose-dependent manner (99 ± 2.0, 91 ± 0.8, 86 ± 3.8 mmHg for control, fima 1.0 and 3.0 mg/kg, respectively, $p < 0.05$, $p < 0.01$). (Fig. 2a).

Fimasartan improved neurological functional outcomes in a dose dependent manner

.

Functional recovery was significantly improved by fimasartan-treated groups (n = 16) compared to the control group (n = 19) at 1h, 1 day and 3 days after ICH. In all rats, the mNSS score was 0 before ICH, which indicated normal neurological functioning. In the control group, the mNSS score peaked (10 ± 0.4) 1 h after ICH and decreased to 7 ± 0.4 on day 3. In the fimasartan-treated groups, the mNSS score also decreased from day 1 to day 3 after ICH compared with the score at the 1h time point in a dose-dependent manner. Compared to the control group, all of the fimasartan-treated groups demonstrated a significant decrease in the mNSS score on all of the time points ($p < 0.001$) (Fig.2b).

For the forelimb placing test, the score was 100 in all the rats before ICH, which indicated normal forelimb function. In the control group, minimal improvement was observed from 1h after ICH (4.7 ± 0.3) to 3 days after ICH (25.6 ± 1.2). In the fimasartan-treated groups, there was improved from day 1 to day 3 compared with 1 h after ICH in a dose-dependent manner. Compare the control group, all of the

fimasartan-treated groups demonstrated a significant increased on day 3 (Con vs. Fima 0.5 mg/kg 25.6 ± 1.2 vs. 33.8 ± 1.2, $p < 0.05$; Con vs. Fima 1.0 mg/kg: 25.6 ± 1.2 vs. 42.3 ± 1.4, $p < 0.01$; Con vs. Fima 3.0 mg/kg 25.6 ± 1.2 vs 62.7 ± 1.4, $p < 0.001$, respectively) (Fig.2c).

Fimasartan attenuated brain water content and hematoma volume

We evaluated the brain water content and hematoma volume 3 days after ICH. Compared to the control group, both low-dose and regular-dose fimasartan-treated groups showed a significant attenuation in the brain water content at 3 day after ICH (Con vs. Fima 0.5 mg/kg: 82.0 ± 0.08% vs. 81.6 ± 0.10%; Con vs. Fima 1.0 mg/kg: 82.0 ± 0.08% vs 81.3 ± 0.35%; Con vs. Fima 3.0 mg/kg: 82.0 ± 0.08% vs 81.5 ± 0.2%; $p < 0.05$) (Fig.2d).

There was no difference in the hemorrhagic lesion volume in the low-dose and regular dose fimasartan 1.0 mg/kg (Con vs. Fima 0.5 mg/kg: 20.41 ± 1.47 mm^3 vs. 17.5 ± 1.55 mm^3; Con vs. Fima 1.0 mg/kg: 20.41 ± 1.47 mm^3 vs. 18.95 ± 1.68 mm^3), which indicated that these doses of fimasartan did not affect bleeding. However, there was decreased in the fimasartan 3.0 mg/kg group (Con vs. Fima 3.0 mg/kg 20.41 ± 1.47 mm^3 vs. 15.71 ± 0.85 mm^3, $p < 0.05$) at 1 day after ICH. (Fig.2e, f).

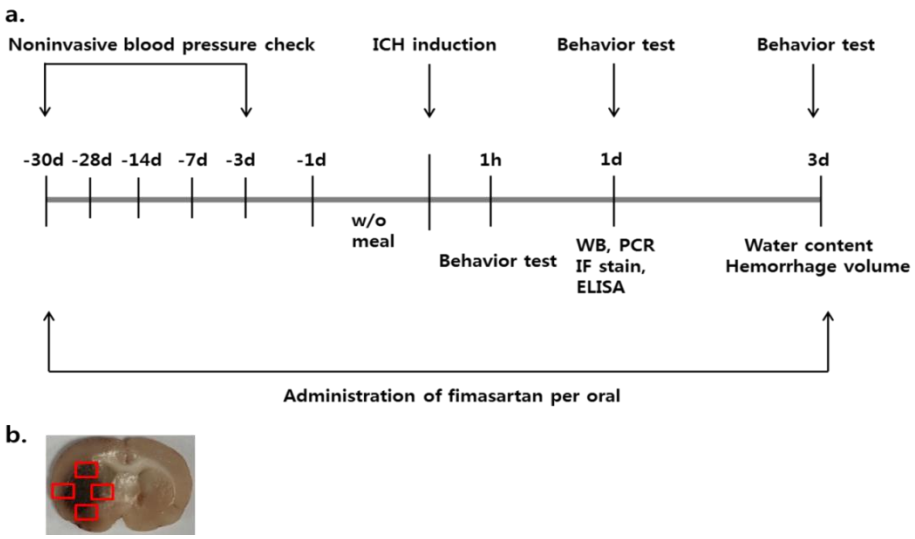

Figure.1 Schematic diagram of the study design and regions of positive cell quantification.

(a) A low-dose (0.5 mg/kg) or regular-dose (1 or 3 mg/kg) of fimasartan or DW was administrated to Sprague-Dawley rats 30 days before the induction of ICH and 2 days after surgery. Noninvasive mean BP was monitored during the pretreatment with fimasartan. Western blot analysis, RT-PCR, ELISA and immunofluorescence staining were performed 1 day after ICH. Brain water content and hemorrhage volume were evaluated 3 days after ICH. The recovery of neurological function was assessed on 1 h, 1 day and 3 days after ICH. **(b)** High-power field images fully covering the perihematomal areas were obtained from slices stained through the center of the hemorrhagic lesion for counting NLRP3 inflammasome components on activated microglia cells. The square markers indicate Iba-1-positive cells in the perihematomal regions.

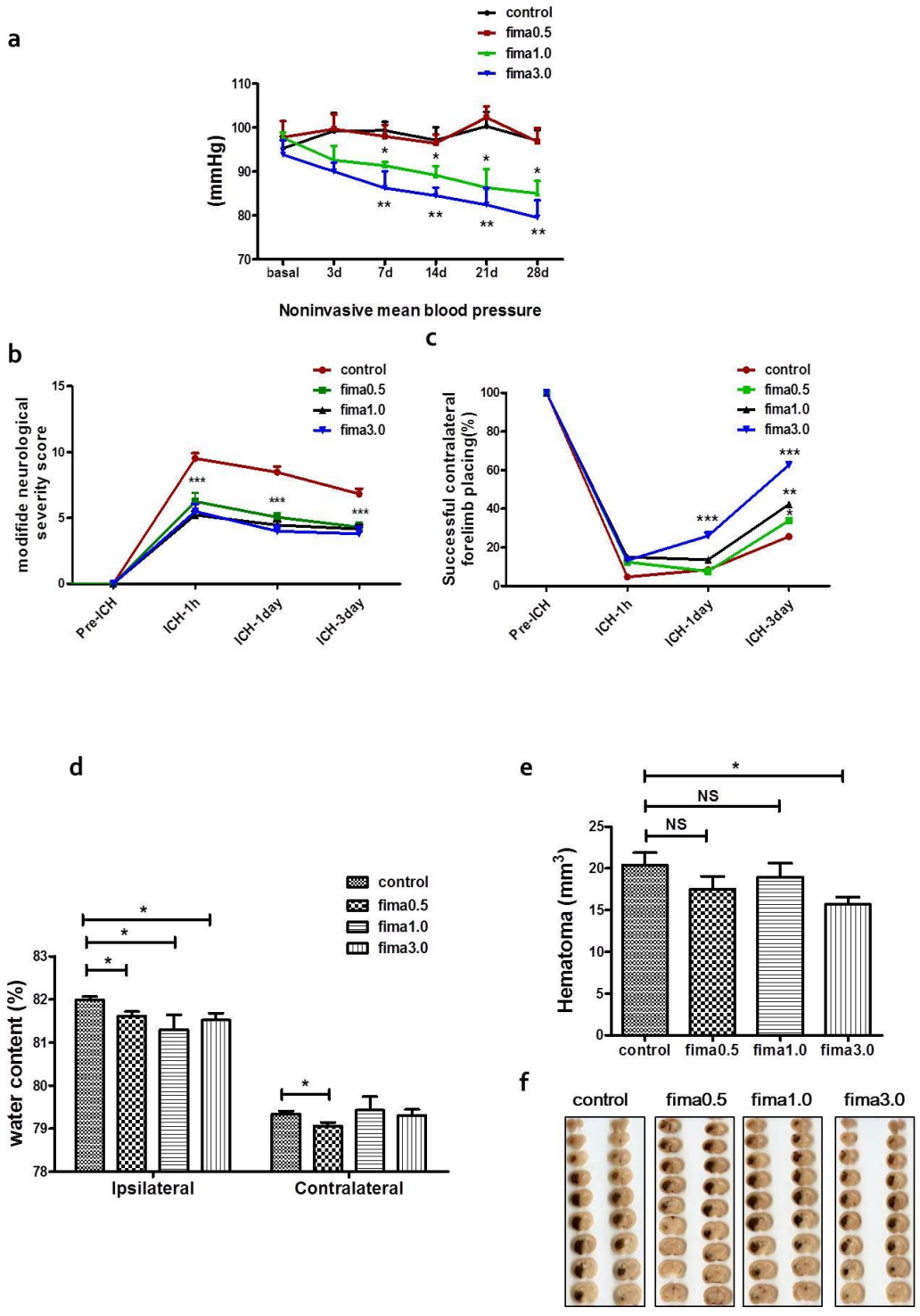
a
control
fima0.5
fima1.0
fima3.0
(mmHg)
basal
3d
7d
14d
21d
28d
Noninvasive mean blood pressure
b
modifide neurological severity score
Pre-ICH
ICH-1h
ICH-1day
ICH-3day
c
Successful contralateral forelimb placing(%)
d
water content (%)
Ipsilateral
Contralateral
e
Hematoma (mm3)
NS
f

Figure. 2 Fimasartan regulated blood pressure, improved neurological functional recovery and attenuated brain water content. Noninvasive mean BP **(a)** were decreased in the regular-dose fimasartan groups at 3 days after the start of fimasartan administration, but in the low-dose fimasartan group, the mean BP were not different from that of the control group (n = 10 per group). Fimasartan improved the neurologic functional discovery in intracerebral hemorrhage (ICH) injury. All rats (n = 16 per group) were subjected to the modified Neurological Severity Score (mNSS) (**b**) and the forelimb placing test **(c)**. The mNSS was 0 and the forelimb placing test scores was 100, indicating normal neurological function. Compared to the control group, **(b)** demonstrated the mNSS was decreased in all of the fimasartan-treated groups from day 1 to day 3 compared with 1h time point after ICH. **(c)** demonstrated the forelimb placing test scores were increased in all of the fimasartan-treated groups from day 1 to day 3 compared with 1h time point after ICH. **(d)** Brain water content of all doses of the fimasartan-treatment groups was lower than control group in the hemorrhagic hemisphere (n = 8 for control group and n = 12 for fimasartan-treatment groups; * $p < 0.05$). **(e, f)** The hemorrhage volumes were not different between the control and low-dose 0.5-mg/kg and regular dose 1.0-mg/kg group. The 3.0-mg/kg group decreased the hemorrhage volume compared with the control group (n = 8 per group; * $p < 0.05$, ** $p < 0.01$, *** $p < 0.001$).

Fimasartan inhibited the activation of NF-κB/IκB and the downstream molecule COX-2

Based on the preliminary experiments, we determined that the low-dose of fimasartan (0.5 mg/kg) was the effective dose, and then investigated the anti-inflammatory mechanism of the low-dose fimasartan effect on ICH rats. We first evaluated the activation of the NF-κB pathway, which is the priming signal for the inflammasome process. Compared to the sham group, NF-κB ($p < 0.05$ compared to Sham) and COX-2 ($p < 0.01$ compared to Sham) were significantly activated, and IκB ($p < 0.05$ compared to Sham) was significantly degraded in the control group. However, these changes were significantly attenuated by long-term pretreatment with low-dose fimasartan (NF-κB: $p < 0.05$ compared to Con; IκB: $p < 0.001$ compared to Con and COX-2: $p < 0.05$ compared to Con) (Fig. 3a, b, c, d).

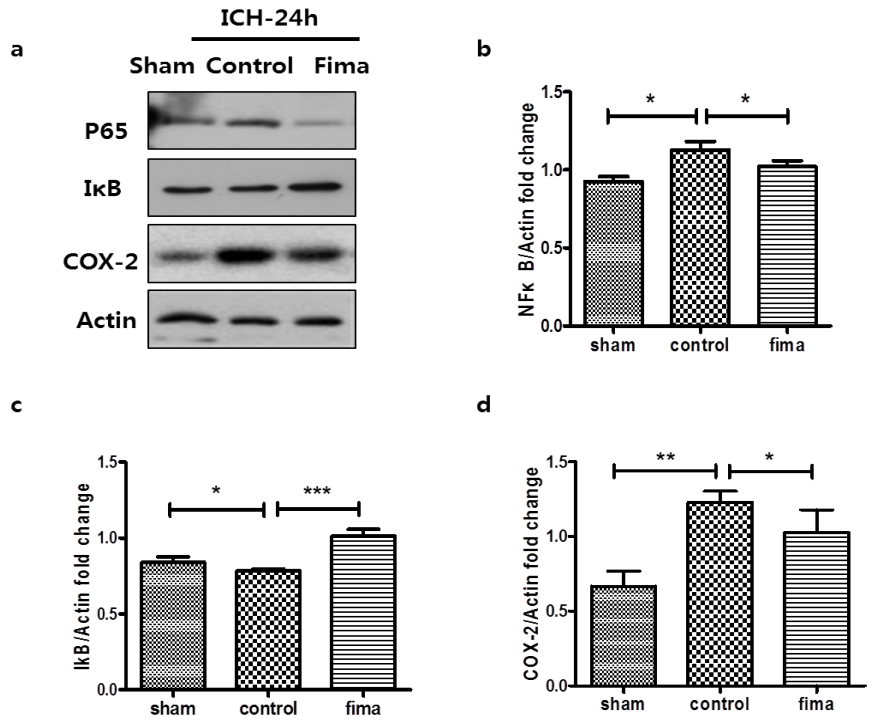

Figure.3 Fimasartan attenuated ICH-induced the NF-κB pathway activation and downstream molecule COX-2.

Twenty-four hours after ICH, the density of NF-κB **(b)** and COX-2 **(d)** in the control group was higher than in the sham group. After long-term administration of low-dose fimasartan, the density in the fimasartan group was lower than in the control group. The density of IκB **(c)** in the control group was lower than in the sham group, and that of the fimasartan group was higher than in the control group. Data are presented as the mean ± SEM from three independent experiments (n = 4 per group; * $p < 0.05$, ** $p < 0.01$, *** $p < 0.001$).

Fimasartan inhibited the activation of NLRP3/ASC/caspase-1 and the subsequent release of IL-1β

We evaluated the expression of the NLRP3/ASC/caspase-1 complex, which is the second inflammatory signal, involved in brain injury after ICH. We further analyzed the role of low-dose fimasartan in the activation of the NLRP3 inflammasome. Compared to their levels in the sham group, NLRP3 ($p < 0.05$ compared to Sham), ASC ($p < 0.001$ compared to Sham) and cleaved caspase-1 ($p < 0.05$ compared to Sham) were significantly upregulated 1 day after ICH in the control group (Fig. 4b, c, d). The production of mature IL-1β ($p < 0.01$ compared to Sham) was also significantly increased (Fig. 4e). However, these effects were significantly inhibited by long-term pretreatment with low-dose fimasartan (NLRP3: $p < 0.01$ compared to Con; ASC: $p < 0.05$ compared to Con; cleaved caspase-1: $p < 0.05$ vs. Con; mature IL-1β: $p < 0.01$ compared to Con).

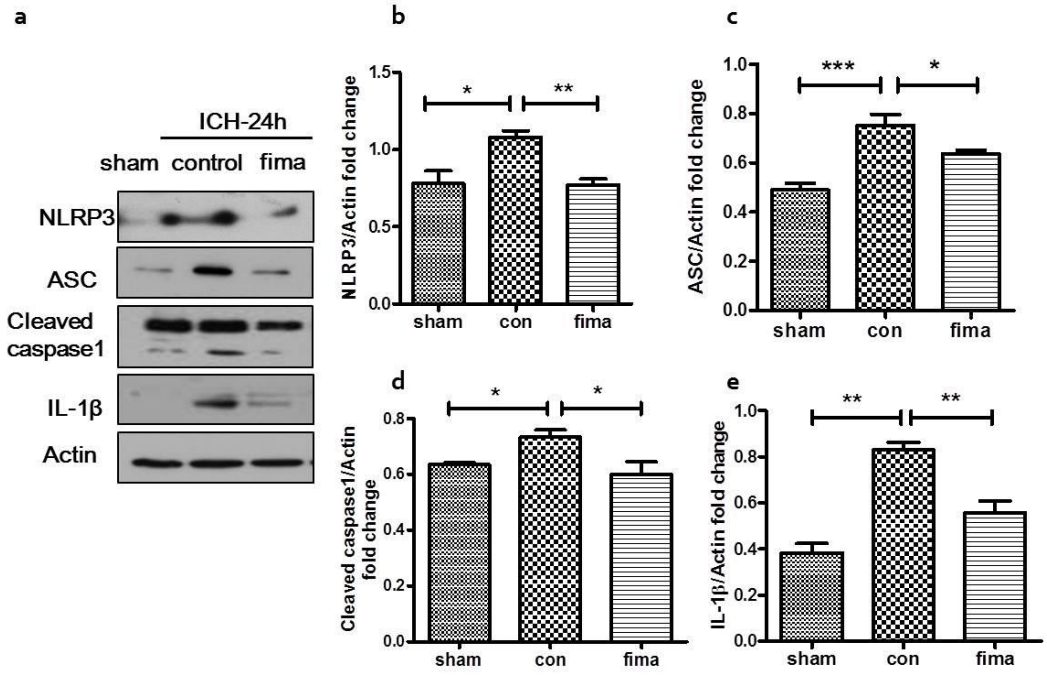

Figure. 4 Fimasartan attenuated ICH-induced NLRP3 inflammasome activation. Twenty-four hours after ICH, the density of NLRP3 **(b)**, ASC **(c)**, caspase-1 **(d)** and IL-1β **(e)** in the control group was higher than in the sham group. After long-term administration of low-dose fimasartan, the density in the fimasartan group was significantly lower than in the control group. Data are presented as the mean ± SEM from three independent experiments. (n = 4 per group; * $p < 0.05$, ** $p < 0.01$, *** $p < 0.001$).

Table 1. List of Antibodies

Antibody	Supplier, Catalog No.	Host	WB	IF
NLRP3	Santa Cruz, sc-66846	rabbit	1:200	1:50
ASC	Santa Cruz, sc-22514	rabbit	1:200	1:100
Caspase-1	Abcam, ab1872	rabbit	1:200	1:50
IL-1ß	Abcam, ab9722	rabbit	1:1000	-
IL-18	Santa Cruz, sc-7954	rabbit	1:200	-
NFκB	Abcam, ab7970	rabbit	1:1,000	-
IκB	Cell Signaling, 9242	rabbit	1:1,000	-
COX-2	Abcam, ab15191	rabbit	1:1,000	-
GFAP	Cell Signaling, 3670	mouse	-	1:200
Iba-1	Santa Cruz, sc-28528	goat	-	1:50
Actin	Bioworld, BSAP0060	rabbit	1:10,000	-

WB, Western Blot; IF, Immunofluorescence

Fimasartan reduced ICH-induced expression of NLRP3 inflammasome mRNA and the subsequent release of pro-inflammatory cytokines

The mRNA levels of NLRP3, ASC and caspase-1 were higher in the ICH group than in the sham group. ICH induced a 0.7-fold increase in NLRP3 mRNA ($p < 0.001$ compared to Sham), a 0.5-fold increase in ASC mRNA ($p < 0.05$ compared to Sham) and a 1.2-fold increase in caspase-1 mRNA ($p < 0.001$ compared to Sham). However, long-term pretreatment with low-dose fimasartan significantly decreased these mRNA expression levels with a 0.3-fold decrease in NLRP3 mRNA ($p < 0.001$ compared to Con), a 0.2-fold decrease in ASC mRNA ($p < 0.05$ compared to Con) and a 0.3-fold decrease in caspase-1 mRNA ($p < 0.001$ compared to Con) (Fig. 5a, b, c). Compared with their secretion in the sham group, the subsequent secretion of the cytokines IL-1β and TNF-α was significantly increased 1 day after ICH in the control group ($p < 0.001$ compared to Sham). Fimasartan effectively reduced the secretion of these cytokines with a 0.2-fold decrease in IL-1β ($p < 0.05$ compared to Con) and a 0.5-fold decrease in TNF-α ($p < 0.001$ compared to Con) (Fig. 5d, e). The data of the RT-PCR and ELISA experiments are summarized in Supplementary Table 2.

Table 2. RT-PCR and ELISA

Antibody	Sham	Control	Fimasartan
RT-PCR			
NLRP3	0.62 ± 0.04	1.03 ± 0.02	0.76 ± 0.03
Caspase1	0.47 ± 0.02	1.02 ± 0.02	0.72 ± 0.03
ASC	0.92 ± 0.15	1.42 ± 0.14	1.09 ± 0.09
ELISA			
IL-1β	5.04 ± 0.54	47.35 ± 2.41	37.95 ± 2.18
TNF-α	6.19 ± 0.61	13.08 ± 0.51	7.05 ± 0.32

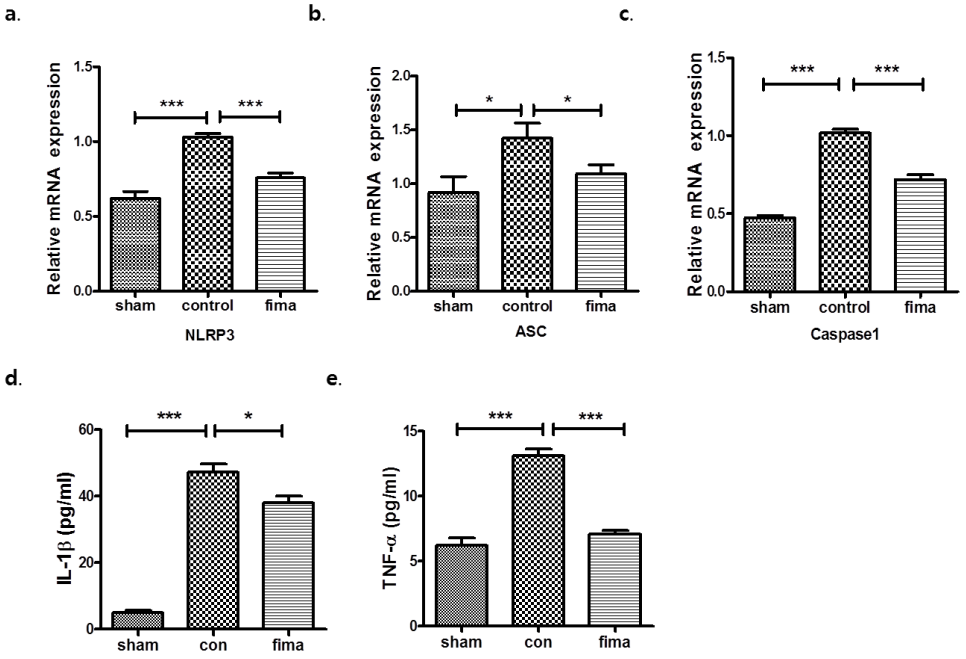

Figure.5 Fimasartan inhibited ICH-induced expression of NLRP3 inflammasome mRNA and release of pro-inflammatory cytokines.

Twenty-four hours after ICH, the mRNA expression of NLRP3 (**a**), ASC (**b**), caspase-1 (**c**) and the release of pro-inflammatory cytokines IL-1β (**d**) and TNF-α (**e**) were higher in the control group than in the sham group. Long-term administration of low-dose fimasartan reduced the expression of NLRP3 mRNA and subsequent release of cytokines. The RT-PCR results are expressed as a fold change relative to the control group. Data are presented as the mean ± SEM from three independent experiments (n= 5 per group; * $p < 0.05$, *** $p < 0.001$).

Fimasartan downregulated ICH-induced NLRP3/ASC/caspase-1 expression in microglia and astrocytes

To determine the expression of inflammasome components on astrocytes and microglia cells, double IF staining were performed (Fig.6-7). The results showed that NLRP3/ASC/caspase-1 inflammasome was predominantly expressed in Iba-1-positive microglia and GFAP-positive astrocytes. The NLRP3 components were significantly increased 1day after ICH in the area around the hematoma in the brain ipsilateral hemisphere compared to the sham group. Long-term treatment with low-dose fimasartan significantly decreased the ICH-induced overexpression of NLRP3/ASC/caspase-1 in target brain cells. The quantitative analysis showed that the fimasartan-treated groups had a decreased number of NLRP3 component-positive cells than the control group. Compare to the control group, in the Iba-1-positive microglia (NLRP3: 124 ± 12 vs. 44 ± 7, $p < 0.01$; ASC: 63 ± 5 vs. 34 ± 3, $p < 0.01$; Caspase-1: 75 ± 6 vs. 33 ± 4, $p < 0.01$) (Fig.6d) and in the GFAP-positive astrocytes (NLRP3:104 ± 16 vs. 57 ± 4, $p < 0.05$; ASC: 93 ± 15 vs. 45 ± 12, $p < 0.05$; Caspase-1: 95 ± 10 vs. 33 ± 7, $p < 0.01$) (Fig.7d).

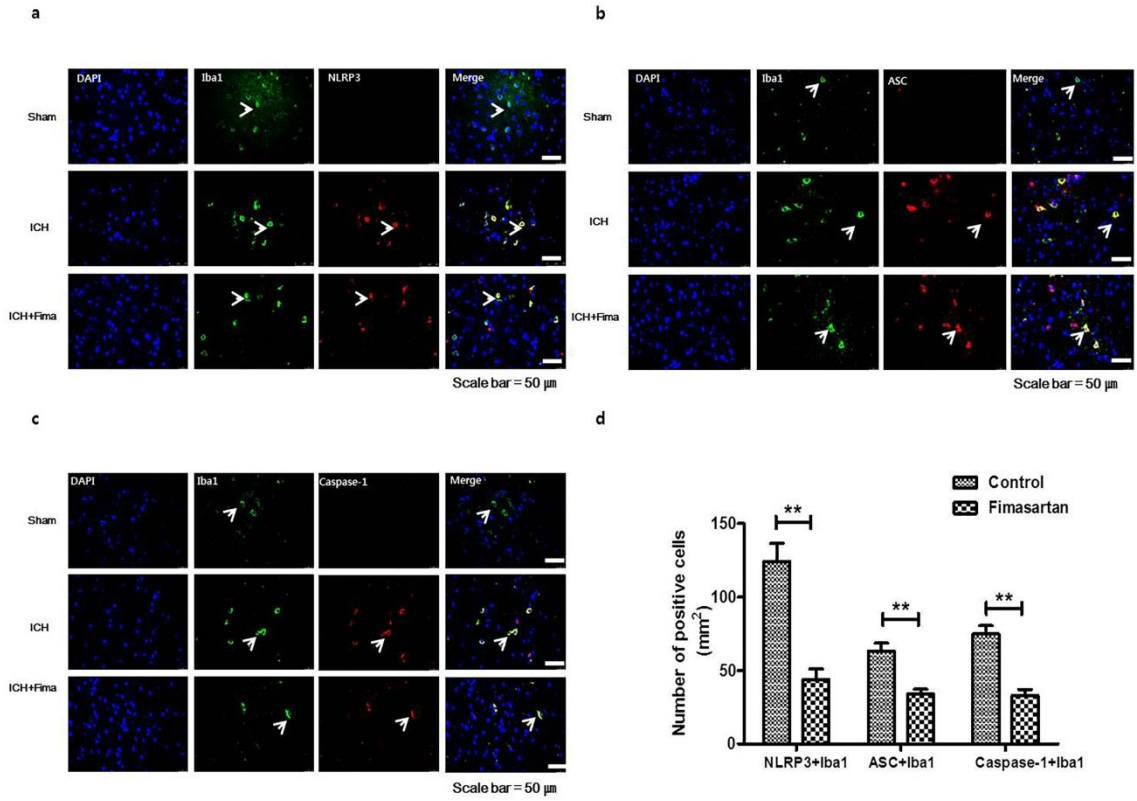

Figure.6 Fimasartan reduced ICH-induced activation of NLRP3 inflammasome in combination with Iba-1-positive microglia.

Double labeling immunofluorescent staining showed co-labelling for NLRP3 and Iba-1**(a)**, ASC and Iba-1(**b**) and Caspase-1 and Iba-1(**c**) after ICH. Quantitative analysis of NLRP3 immunoreactivity in the microglia expressed as a number of NLRP3/ASC/Caspase-1 and Iba-1 positive cells **(d)**. An increased in the proportion of area positively stained with Iba-1 antibody was used to measure of microglia activation. Data are presented as mean ± SEM. Scale bar = 50 ㎛. (n= 5 per group; ** $p < 0.01$).

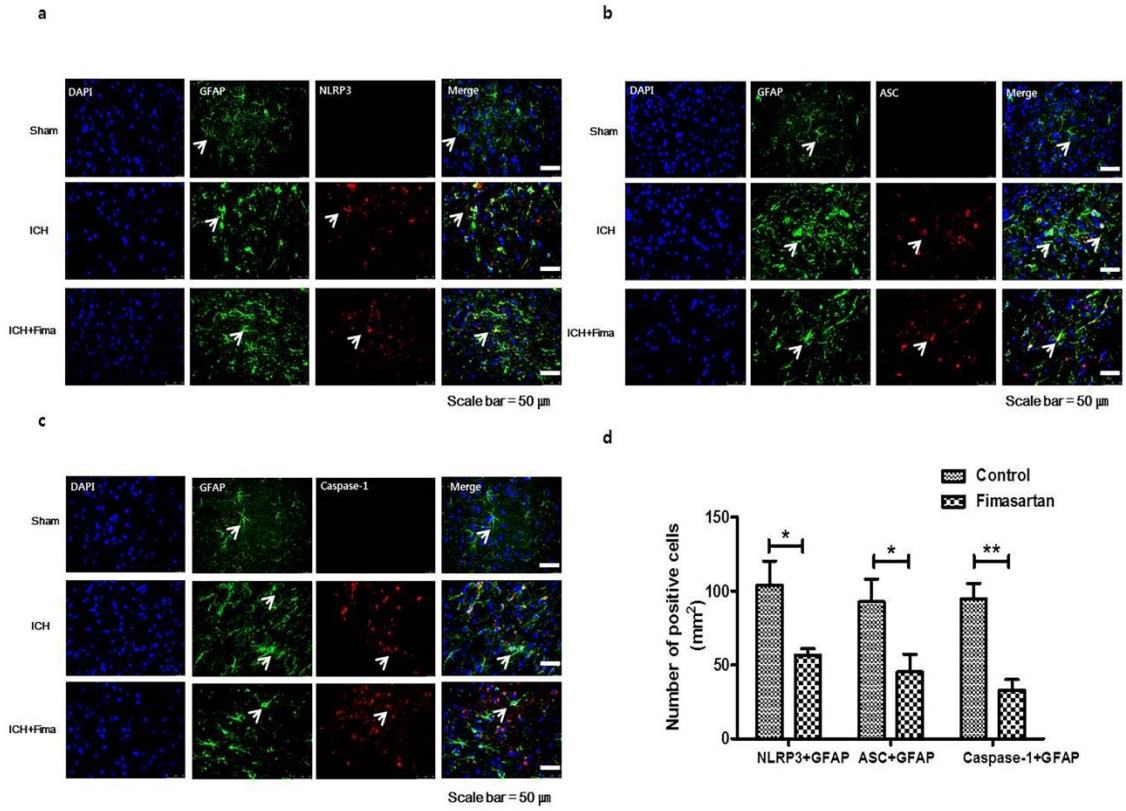

Figure.7 Fimasartan reduced ICH-induced activation of NLRP3 inflammasome in combination with GFAP-positive astrocytes.

Double labeling immunofluorescent staining showed co-labelling for NLRP3 and GFAP (**a**), ASC and GFAP (**b**) and Caspase-1 and GFAP (**c**) after ICH. Quantitative analysis of NLRP3 immunoreactivity in the astrocytes expressed as a number of NLRP3/ ASC/Caspase-1 and GFAP positive cells (**d**). An increased in the proportion of area positively stained with GFAP antibody was used to measure of astrocytes activation. Data are presented as mean ± SEM. Scale bar = 50 μm (n= 5 per group; * $p < 0.05$, ** $p < 0.01$).

Fimasartan inhibits hemolysate-induced NFκB activity in astrocytes

We detected the role of fimasartan in hemolysate-induced nuclear translocation and mRNA expression of NFκB in astrocytes. Cells were incubated in the absence or presence of fimasartan for 12 h, followed by exposure to hemolysate for 1 h. Astrocytes nuclear protein was extracted, and then the NFκB (p65) translocation was assessed by western blot. As shown in Fig. 8a, fimasartan suppressed nuclear translocation of p65 by 1.3-fold compared with the hemolysate alone group ($p < 0.05$). Because p65 and p50 are the major units of NFκB in astrocytes and neurons, we further observed the role of fimasartan on hemolysate-induced activation of NFκB1 (P50) mRNA expression. Astrocytes were treated in the absence or presence of fimasartan for 12 h, stimulated with hemolysate for 30 min, and then NFκB1 (P50) mRNA expression was analyzed by real-time RT-PCR. The level of P50 also was markedly inhibited (164-fold) compared with the hemolysate alone group ($p < 0.01$; Fig. 8b).

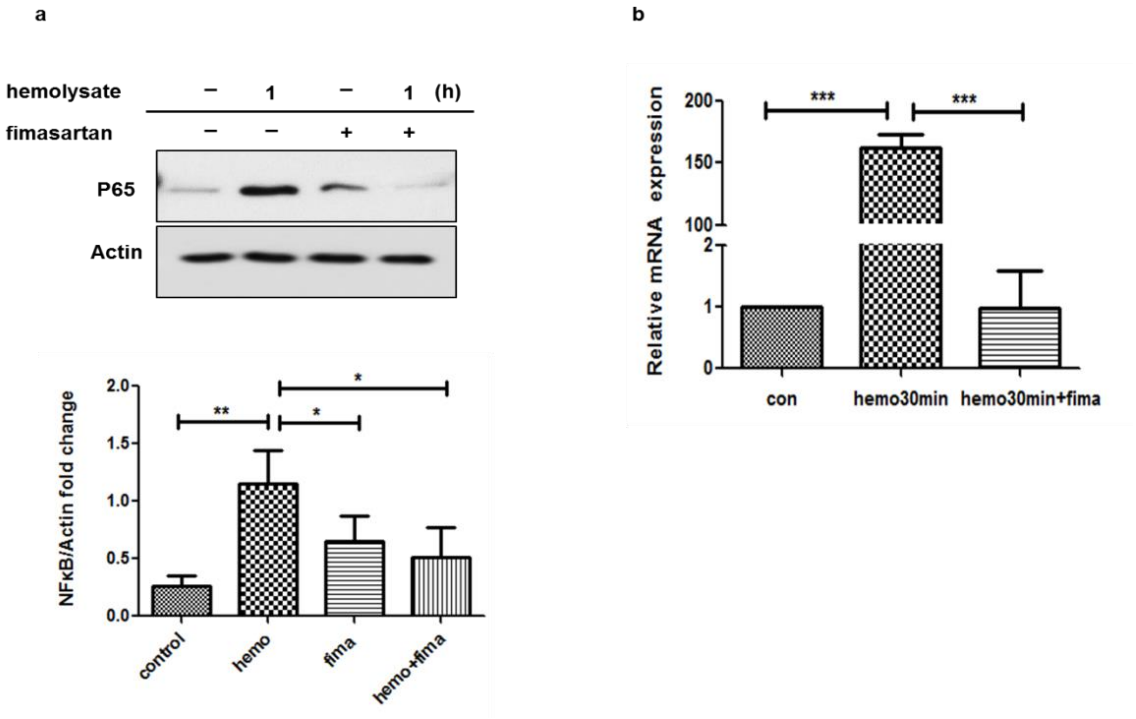

Figure.8 Fimasartan inhibited the hemolysate-induced nuclear-translocation of NFκB and mRNA expression in astrocytes. The cells were divided into 4 groups. One is a control group. The second group was treated with hemolysate for 1 h. The third group was pretreated with fimasartan alone and the last was incubated with hemolysate after pretreatment with fimasartan. NFκB (p65) activity was observed by western blotting. **(a)** Quantification was determined by scanning densitometry of bands and standardized with β-actin. **(b)** Astrocytes were divided into 3 groups. One is a control group and the second group was treated with hemolysate for 30 min. The third group was incubated with hemolysate after pretreatment with fimasartan. The expression of NFκB mRNA was assessed by real-time RT-PCR. Values indicate the mean ± SD of at least three independent experiments. (** $P < 0.01$, * $P < 0.05$, *** $P < 0.001$)

Fimasartan suppresses the hemolysate-induced COX-2 expression and IL-1β production

To evaluate mechanism underlying the inflammatory response to hemolysate, we treated astrocytes with 10% hemolysate to induce inflammatory activity. Upregulation of inflammatory cytokine IL-1β were observed when compared with control group. After 12 h of fimasartan pretreatment, there was a significant decrease in COX-2 expression as shown by the immunoblot (Fig. 9a) and RT-PCR analysis (Fig. 9b). As shown by the immunoblot, hemolysate-induced expression of COX-2 was increased by 43% at 6 h ($p < 0.01$) and by 51% at 12 h ($p < 0.01$) compared with the control group. However, after 12 h of pretreatment with fimasartan, COX-2 expression was dramatically decreased by 21% ($p < 0.01$) at 6 h and by 11% at 12 h ($p < 0.05$) compared with the hemolysate alone treatment group. To determine whether the modulation of inflammation by fimasartan was related to COX-2 gene expression, we analyzed the hemolysate-induced mRNA expression of COX-2. Astrocytes were pretreated fimasartan in a dose-dependent manner for 12 h before incubation with hemolysate. As shown in Fig. 9b, the expression of COX-2 mRNA was increased by 72% after stimulation with hemolysate compared with the control group ($p < 0.01$). This increase was consistently downregulated by treatment with fimasartan in a dose-dependent manner. When fimasartan was added at 10, 30 and 100 ng/mL, COX-2 expression decreased by approximately 4%, 10% and 40%, respectively, when compared with the hemolysate alone treatment group (Fig. 9b). These data indicated that at a high concentration (100ng/ml), fimasartan clearly inhibited the induction of COX-2 mRNA ($p < 0.01$). Consistent with the data demonstrated above, hemolysate induced much stronger (68.8% compared with control group, $p < 0.01$) inflammatory cytokine IL-1β release. After fimasartan treatment at the indicated concentrations, IL-1β levels *consistently* decreased by 17%, 26%, ($p < 0.05$), 64% ($p < 0.01$) and 154% ($p < 0.01$), when compared with the hemolysate alone treatment group (Fig. 9c).

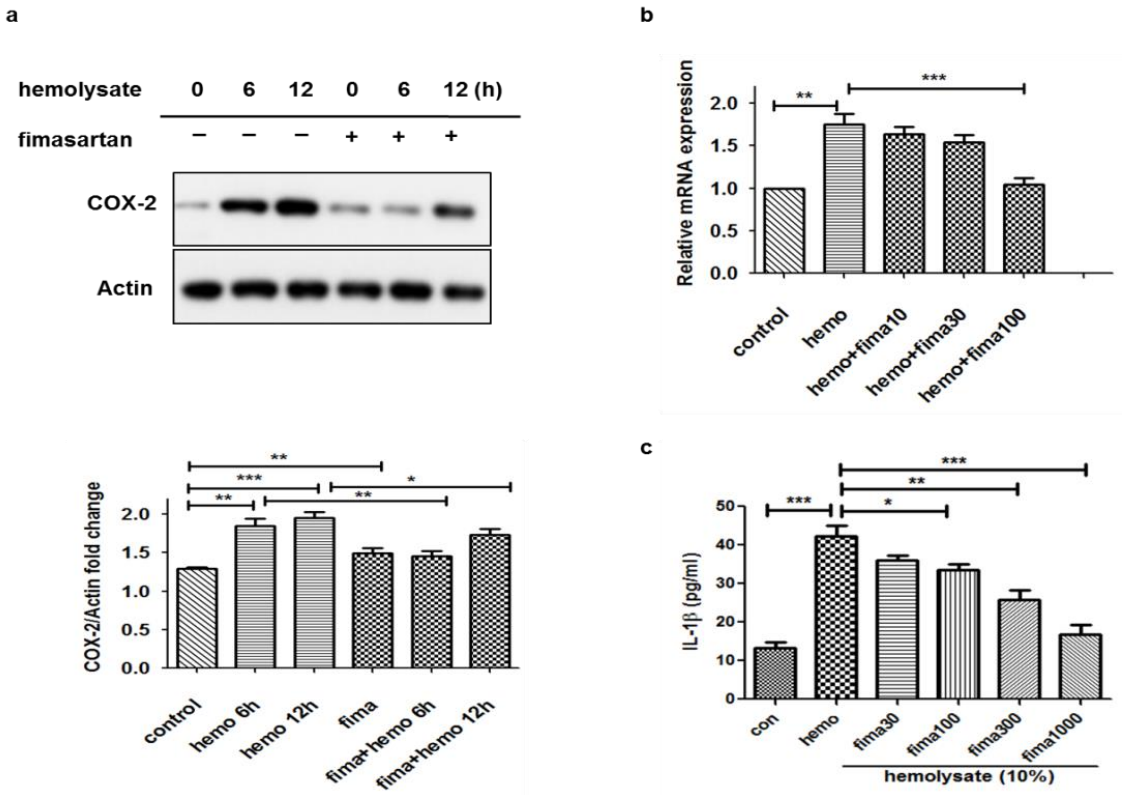

Figure.9 Fimasartan inhibited the expression of the COX-2 and IL-1β in astrocytes. The cells were divided into 4 groups. One is the control group and the second group was treated with hemolysate. The third group was pretreated with fimasartan alone and the last was incubated with hemolysate after pretreatment with fimasartan. Inhibition of COX-2 was observed by western blotting. **(a)** Quantification was determined by scanning densitometry of bands and standardized with β-actin. **(b)** Astrocytes were pretreated with or without different concentrations of fimasartan and then incubated in the presence or absence of hemolysate for 18 h. The expression of COX-2 was assessed by real-time RT-PCR. **(c)** The expression of IL-1β was assessed by ELISA. Values indicate the mean ± SD of at least three independent experiments. ** $P < 0.01$, * $P < 0.05$, *** $P < 0.001$; Fima stands for fimasartan and hemo stands for hemolysate.

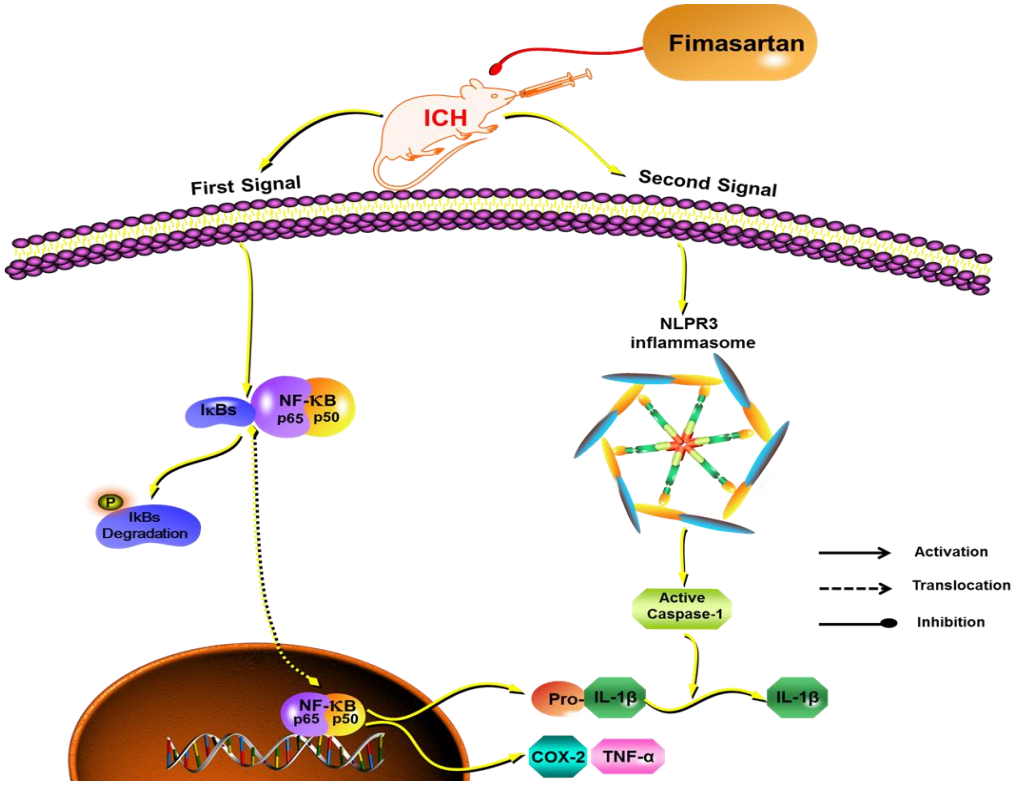

Figure.10 A hypothetical mechanism of the fimasartan attenuates the NLRP3 inflammasome activation to ICH. ICH induces inflammatory response of microglia and astrocytes via activating 2 signals. The priming signal, that is NF-κB pathway, releases the cytokines pro-IL-1β and TNFα. The second signal assembles the NLRP3 inflammasome and cleaved into the active caspase-1, which subsequently promotes the pro-IL-1β into the mature cytokine IL-1β. Long treatment of low-dose fimasartan reduces the secondary damage induced by acute ICH via down-regulating the activation of NF-κB pathway and NLRP3 inflammasome.

DISCUSSION

Long-term pretreatment with low-does fimasartan improved the outcome of ICH stroke and inhibit ed the inflammatory response related with the secondary damage of ICH. Our study suggested that the components of the NLRP3 inflammasome are involved in the inflammation following ICH, and prestroke treatment with the low-dose fimasartan protected against the damage by inhibiting the activation of NLRP3 inflammasome without lowering the BP on ICH rats.

Inflammation-induced by ICH is considered a key mechanism responsible for the secondary brain damage of ICH. Recently the inflammasome has been recognized as a vital player in the innate immune response in stroke (22). The inflammasome has been considered to be a milestone in the immunology since it was discovered in 2002 (40). Subsequently, many studies reported that the inflammasome is involved in a variety of inflammatory diseases ranging from inflammatory bowel disease to auto-inflammatory disease (41-43). NLRP3 is the most intensively studied inflammasome and has been broadly investigated in the CNS immune system, especially involved in the ICH-induced inflammatory response (12, 23). NLRP3 contributes to the processing of IL-1β, which is also an important therapeutic target in ICH (44). This raises the hypothesis that targeting the formation of the NLRP3 inflammasome may be a potential therapy for ICH. Therefore, in this study, we focused on fimasartan treatment on ICH by inhibiting the two signals of processing IL-1β. Consistent with our hypothesis, both the two signals was activated on 1 day post-ICH. ~~Furthermore,~~ And low-dose fimasartan ameliorated these activations without affecting the BP, which suggests that the anti-inflammasome effects of low-dose fimasartan are independent of its effect on BP. Furthermore, inhibition of inflammasome activation by fimasartan was associated with a recovery of neurological function and a reduction of brain edema.

The classical immune cells of the CNS are associated with the inflammatory response after ICH. It is well known that the activation of these cells results in release of inflammatory cytokines such as TNF-α and IL-1β, destruction of the BBB and ~~subsequently,~~ the promotion of edema within the first 24 h (11). Different types of inflammasome in the CNS generate innate immune inflammatory responses in

astrocytes and microglia (45, 46). Accumulating evidences suggest that the NLRP3 inflammasome was found to activate in the microglia (46). As well-known, Microglia is the resident macrophage in the brain and has an important role of modulating inflammatory response induced by ICH. The microglial activation mostly happens on 24 h of ICH and the amelioration of immune response in the acute stage of ICH could be neuroprotective effect. Previous studies demonstrated that NLRP3 proteins, especially the IL-1β, strongly increased in 24 h in stroke models (47, 48).Therefore In this study, we selected the 24 h as the target time point of inflammatory induced by ICH. Except microglia, activation astrocytes also express the inflammasome and enhance the ICH induced brain damage (49). In this study, double-labeled immunostaining suggests high expressions of NLRP3/ASC/Caspase-1 complex colocalized with the activate microglia and astrocytes on the acute stage of ICH rat model.

ARBs have been proven to have pleiotropic neuroprotective effects in numerous pre-clinical studies. A recent study indicated that telmisartan has neuroprotective effects by inhibiting activation of inflammasome in a stroke-resistant spontaneously hypertensive rat model (50). Fimasartan has a stronger affinity for the AT1 receptor subtype inside the blood brain barrier, and was found to have neuroprotective effects for ischemic disease. Brain penetration of telmisartan and candesartan were indicated in previous studies (51, 52), therefore we speculate fimasartan, as one of ARBs, could have the ability to enter through the BBB.

In our previous study, we found that fimasartan ameliorated the hemolyste-induced immune response on astrocytes by inhibiting the activation of NF-κB pathway (29). Of translational significance, we investigated the effects of fimasartan in an ICH rat model. In the present study, fimasartan was orally pre-administered at the low and regular dose to normotensive rats for one month prior and 2 days after induction of ICH. All doses of fimasartan effectively decreased the brain water content and improved the functional recovery. Moreover, the BP in the low dose fimasartan was not affected. To explore the neuroprotective effects of fimasartan independent of regulating BP, we evaluated the effects of extended treatment with low-dose fimasartan on ICH. We found that low-dose fimasartan inhibited the activity of the inflammasome without lowing BP. Compare to previous studies on low dose ARBs (27, 53), this study supported that prestroke use of low-dose fimasartan has favorable effects on acute ICH

injury without affecting BP. Although fimasartan is one of novel ARBs mainly used as anantihypertensive medication, we think low-dose fimasartan may confer preventive and therapeutic effects on ICH in addition to its effect on BP. By targeting the NLRP3 inflammasome, future studies should investigate strategies using ARBs to offer novel therapies for ICH.

Astrocytes play a key role in the process of inflammation in the cerebral nervous system (54). In the vitro experiment, we observed that astrocytes exposed to hemolysate activate the classical inflammation signaling pathways. Several reviews have shown that astrocytes participate in innate immunity by releasing cytokines and chemokines. NF-κB is a significant transcription factor and a key regulator of inflammatory genes; blocking the NF-κB pathway has anti-inflammatory effects. The NF-κB pathway mediated by Toll-like receptors, as the priming signal, produce the pro-IL-1β and potentially other inflammasome components (55). Our research shows that blocking the NF-κB pathway in astrocytes consistently inhibits the gene expression of COX-2. NF-κB translocates to the nucleus where it activates the inflammatory response only after IκB kinase degradation. In previous study, we confirmed fimasartan inhibits IκB kinase degradation in astrocytes (29).

COX-2 is one of the enzymes important for regulating the inflammatory process. Suppressing the expression of COX-2 may be important for anti-inflammatory activities. The hemolysate-induced upregulation of COX-2 and iNOS mRNA levels have been previously reported (8). NF-κB is involved in the regulation of COX-2 expression. Recently, it has been shown that fimasartan inhibits iNOS via the attenuation of NF-κB in macrophages (56). Our study shows that the over-expression of COX-2 in astrocytes, which is associated with the nuclear-translocation of NF-κB, can be reversed by pretreatment with fimasartan in a dose-dependent manner (Fig. 4). These results suggest that fimasartan inhibits COX-2 expression by inhibiting the nuclear-tranlocation of NF-κB.

CONCLUSION

In summary, this study showed that the activation of the NLRP3/ASC/caspase-1 inflammasome and the subsequent cytokines, IL-1β and TNF-α, are involved in the secondary damage of ICH. By inhibiting the NLRP3 inflammasome, the long-term pretreatment with low-dose fimasartan is a potential therapeutic strategy to protect from secondary damage of acute ICH. Further clinical studies are necessary to confirm the neuroprotective effects of fimasartan on ICH.

REFERENCES

1. Keep RF, Hua Y, Xi G. Intracerebral haemorrhage: mechanisms of injury and therapeutic targets. The Lancet Neurology.11(8):720-31.

2. Qureshi AI, Mendelow AD, Hanley DF. Intracerebral haemorrhage. The Lancet.373(9675):1632-44.

3. Qureshi AI, Tuhrim S, Broderick JP, Batjer HH, Hondo H, Hanley DF. Spontaneous Intracerebral Hemorrhage. New England Journal of Medicine. 2001;344(19):1450-60.

4. Sasaki T, Kasuya H, Onda H, Sasahara A, Goto S, Hori T, et al. Role of p38 mitogen-activated protein kinase on cerebral vasospasm after subarachnoid hemorrhage. Stroke. 2004;35(6):1466-70.

5. Edye ME, Lopez-Castejon G, Allan SM, Brough D. Acidosis drives damage-associated molecular pattern (DAMP)-induced interleukin-1 secretion via a caspase-1-independent pathway. Journal of Biological Chemistry. 2013;288(42):30485-94.

6. Lu H, Shi J-X, Zhang D-M, Shen J, Lin Y-X, Hang C-H, et al. Hemolysate-induced expression of intercellular adhesion molecule-1 and monocyte chemoattractant protein-1 expression in cultured brain microvascular endothelial cells via through ros-dependent nf-κb pathways. Cellular and molecular neurobiology. 2009;29(1):87-95.

7. Gong C, Boulis N, Qian J, Turner DE, Hoff JT, Keep RF. Intracerebral hemorrhage-induced

neuronal death. Neurosurgery. 2001;48(4):875-83.

8. Lu H, Shi J-X, Zhang D-M, Wang H-D, Hang C-H, Chen H-L, et al. Inhibition of hemolysate-induced iNOS and COX-2 expression by genistein through suppression of NF-κB activation in primary astrocytes. Journal of the neurological sciences. 2009;278(1):91-5.

9. Lu H, Shi J-X, Zhang D-M, Chen H-L, Qi M, Yin H-X. Genistein, a soybean isoflavone, reduces the production of pro-inflammatory and adhesion molecules induced by hemolysate in brain microvascular endothelial cells. Acta neurologica Belgica. 2009;109(1):32.

10. Iadecola C, Anrather J. The immunology of stroke: from mechanisms to translation. Nature medicine. 2011;17(7):796-808.

11. Wang J, Doré S. Inflammation after intracerebral hemorrhage. Journal of Cerebral Blood Flow and Metabolism. 2007;27(5):894-908.

12. Feng L, Chen Y, Ding R, Fu Z, Yang S, Deng X, et al. P2X7R blockade prevents NLRP3 inflammasome activation and brain injury in a rat model of intracerebral hemorrhage: involvement of peroxynitrite. Journal of Neuroinflammation. 2015;12(1):1-17.

13. Meng X-F, Tan L, Tan M-S, Jiang T, Tan C-C, Li M-M, et al. Inhibition of the NLRP3 inflammasome provides neuroprotection in rats following amygdala kindling-induced status epilepticus. Journal of neuroinflammation. 2014;11(1):212.

14. Heneka MT, Kummer MP, Latz E. Innate immune activation in neurodegenerative disease. Nat Rev Immunol. 2014;14.

15. Heneka MT, Kummer MP, Stutz A, Delekate A, Schwartz S, Vieira-Saecker A, et al. NLRP3 is activated in Alzheimer's disease and contributes to pathology in APP/PS1 mice. Nature. 2013;493(7434):674-8.

16. Strowig T, Henao-Mejia J, Elinav E, Flavell R. Inflammasomes in health and disease. Nature. 2012;481.

17. Schroder K, Tschopp J. The inflammasomes. Cell. 2010;140(6):821-32.

18. Dostert C, Pétrilli V, Van Bruggen R, Steele C, Mossman BT, Tschopp J. Innate immune activation through Nalp3 inflammasome sensing of asbestos and silica. Science. 2008;320(5876):674-7.

19. Petrilli V, Papin S, Dostert C, Mayor A, Martinon F, Tschopp J. Activation of the NALP3 inflammasome is triggered by low intracellular potassium concentration. Cell Death & Differentiation. 2007;14(9):1583-9.

20. Mariathasan S, Weiss DS, Newton K, McBride J, O'Rourke K, Roose-Girma M, et al. Cryopyrin activates the inflammasome in response to toxins and ATP. Nature. 2006;440(7081):228-32.

21. Franchi L, Munoz-Planillo R, Nunez G. Sensing and reacting to microbes through the inflammasomes. Nat Immunol. 2012;13(4):325-32.

22. Fann DY-W, Lee S-Y, Manzanero S, Chunduri P, Sobey CG, Arumugam TV. Pathogenesis of acute stroke and the role of inflammasomes. Ageing research reviews. 2013;12(4):941-66.

23. Ma Q, Chen S, Hu Q, Feng H, Zhang JH, Tang J. NLRP3 inflammasome contributes to

inflammation after intracerebral hemorrhage. Annals of neurology. 2014;75(2):209-19.

24. Gallinat S, Yu M, Dorst A, Unger T, Herdegen T. Sciatic nerve transection evokes lasting up-regulation of angiotensin AT2 and AT1 receptor mRNA in adult rat dorsal root ganglia and sciatic nerves. Brain research Molecular brain research. 1998;57(1):111-22.

25. Saavedra JM. Angiotensin II AT1 receptor blockers as treatments for inflammatory brain disorders. Clinical Science. 2012;123(10):567-90.

26. Timaru-Kast R, Wyschkon S, Luh C, Schaible E-V, Lehmann F, Merk P, et al. Delayed inhibition of angiotensin II receptor type 1 reduces secondary brain damage and improves functional recovery after experimental brain trauma. Critical care medicine. 2012;40(3):935-44.

27. Tsukuda K, Mogi M, Iwanami J, Min L-J, Sakata A, Jing F, et al. Cognitive deficit in Amyloid-β–injected mice was improved by pretreatment with a low dose of telmisartan partly because of peroxisome proliferator-activated receptor-γ activation. Hypertension. 2009;54(4):782-7.

28. Kim JH, Lee JH, Paik SH, Kim JH, Chi YH. Fimasartan, a novel angiotensin II receptor antagonist. Archives of pharmacal research. 2012;35(7):1123-6.

29. Yang XL, Kim CK, Kim TJ, Sun J, Rim D, Kim YJ, et al. Anti-inflammatory effects of fimasartan via Akt, ERK, and NFkappaB pathways on astrocytes stimulated by hemolysate. Inflamm Res. 2016;65(2):115-23.

30. Kim CK, Yang XL, Kim YJ, Choi IY, Jeong HG, Park HK, et al. Effect of Long-Term Treatment with Fimasartan on Transient Focal Ischemia in Rat Brain. Biomed Res Int. 2015;2015:295925.

31. Sundboll J, Schmidt M, Horvath-Puho E, Christiansen CF, Pedersen L, Botker HE, et al. Preadmission use of ACE inhibitors or angiotensin receptor blockers and short-term mortality after stroke. Journal of neurology, neurosurgery, and psychiatry. 2015;86(7):748-54.

32. Ciocoiu M, Badescu L, Miron A, Badescu M. The involvement of a polyphenol-rich extract of black chokeberry in oxidative stress on experimental arterial hypertension. Evid Based Complement Alternat Med. 2013;2013:912769.

33. Kurtz TW, Griffin KA, Bidani AK, Davisson RL, Hall JE. Recommendations for blood pressure measurement in humans and experimental animals: part 2: blood pressure measurement in experimental animals: a statement for professionals from the Subcommittee of Professional and Public Education of the American Heart Association Council on High Blood Pressure Research. Arterioscler Thromb Vasc Biol. 2005;25(3):e22-33.

34. Xi G, Keep RF, Hoff JT. Mechanisms of brain injury after intracerebral haemorrhage. Lancet Neurol. 2006;5(1):53-63.

35. Song EC, Chu K, Jeong SW, Jung KH, Kim SH, Kim M, et al. Hyperglycemia exacerbates brain edema and perihematomal cell death after intracerebral hemorrhage. Stroke. 2003;34(9):2215-20.

36. Kim CK, Ryu WS, Choi IY, Kim YJ, Rim D, Kim BJ, et al. Detrimental effects of leptin on intracerebral hemorrhage via the STAT3 signal pathway. Journal of cerebral blood flow and metabolism : official journal of the International Society of Cerebral Blood Flow and Metabolism.

2013;33(6):944-53.

37. Chen J, Li Y, Wang L, Zhang Z, Lu D, Lu M, et al. Therapeutic benefit of intravenous administration of bone marrow stromal cells after cerebral ischemia in rats. Stroke. 2001;32(4):1005-11.

38. Benicky J, Sanchez-Lemus E, Honda M, Pang T, Orecna M, Wang J, et al. Angiotensin II AT1 receptor blockade ameliorates brain inflammation. Neuropsychopharmacology. 2011;36(4):857-70.

39. Jung KH, Chu K, Jeong SW, Han SY, Lee ST, Kim JY, et al. HMG-CoA Reductase Inhibitor, Atorvastatin, Promotes Sensorimotor Recovery, Suppressing Acute Inflammatory Reaction After Experimental Intracerebral Hemorrhage. Stroke. 2004;35(7):1744-9.

40. Martinon F, Burns K, Tschopp J. The Inflammasome: A Molecular Platform Triggering Activation of Inflammatory Caspases and Processing of proIL-β. Molecular Cell. 2002;10(2):417-26.

41. dos Santos G, Kutuzov MA, Ridge KM. The inflammasome in lung diseases. Am J Physiol Lung Cell Mol Physiol. 2012;303(8):L627-33.

42. Villani A-C, Lemire M, Fortin G, Louis E, Silverberg MS, Collette C, et al. Common variants in the NLRP3 region contribute to Crohn's disease susceptibility. Nature genetics. 2009;41(1):71-6.

43. Halle A, Hornung V, Petzold GC, Stewart CR, Monks BG, Reinheckel T, et al. The NALP3 inflammasome is involved in the innate immune response to amyloid-β. Nature immunology. 2008;9(8):857-65.

44. Lok J, Zhao S, Leung W, Seo JH, Navaratna D, Wang X, et al. Neuregulin-1 effects on

endothelial and blood–brain barrier permeability after experimental injury. Translational stroke research. 2012;3(1):119-24.

45. Santoni G, Cardinali C, Morelli MB, Santoni M, Nabissi M, Amantini C. Danger- and pathogen-associated molecular patterns recognition by pattern-recognition receptors and ion channels of the transient receptor potential family triggers the inflammasome activation in immune cells and sensory neurons. Journal of Neuroinflammation. 2015;12(1):1-10.

46. de Rivero Vaccari JP, Dietrich WD, Keane RW. Activation and regulation of cellular inflammasomes: gaps in our knowledge for central nervous system injury. Journal of cerebral blood flow and metabolism : official journal of the International Society of Cerebral Blood Flow and Metabolism. 2014;34(3):369-75.

47. Tomura S, de Rivero Vaccari JP, Keane RW, Bramlett HM, Dietrich WD. Effects of therapeutic hypothermia on inflammasome signaling after traumatic brain injury. Journal of cerebral blood flow and metabolism : official journal of the International Society of Cerebral Blood Flow and Metabolism. 2012;32(10):1939-47.

48. Abulafia DP, de Rivero Vaccari JP, Lozano JD, Lotocki G, Keane RW, Dietrich WD. Inhibition of the inflammasome complex reduces the inflammatory response after thromboembolic stroke in mice. Journal of cerebral blood flow and metabolism : official journal of the International Society of Cerebral Blood Flow and Metabolism. 2009;29(3):534-44.

49. Johann S, Heitzer M, Kanagaratnam M, Goswami A, Rizo T, Weis J, et al. NLRP3

inflammasome is expressed by astrocytes in the SOD1 mouse model of ALS and in human sporadic ALS patients. Glia. 2015;63(12):2260-73.

50. Kono S, Kurata T, Sato K, Omote Y, Hishikawa N, Yamashita T, et al. Neurovascular protection by telmisartan via reducing neuroinflammation in stroke-resistant spontaneously hypertensive rat brain after ischemic stroke. Journal of Stroke and Cerebrovascular Diseases. 2015;24(3):537-47.

51. Michel MC, Foster C, Brunner HR, Liu L. A systematic comparison of the properties of clinically used angiotensin II type 1 receptor antagonists. Pharmacol Rev. 2013;65(2):809-48.

52. Noda A, Fushiki H, Murakami Y, Sasaki H, Miyoshi S, Kakuta H, et al. Brain penetration of telmisartan, a unique centrally acting angiotensin II type 1 receptor blocker, studied by PET in conscious rhesus macaques. Nuclear medicine and biology. 2012;39(8):1232-5.

53. Shimamura M, Nakagami H, Shimosato T, Moritani T, Nakagami F, Kiomy Osako M, et al. Irbesartan improves endothelial dysfunction, abnormal lipid profile, proteinuria and liver dysfunction in Zucker diabetic fatty rats independent of glucose and insulin levels. Experimental and therapeutic medicine. 2011;2(5):957-61.

54. Dong Y, Benveniste EN. Immune function of astrocytes. Glia. 2001;36(2):180-90.

55. Trendelenburg G. Molecular regulation of cell fate in cerebral ischemia: role of the inflammasome and connected pathways. Journal of Cerebral Blood Flow & Metabolism. 2014;34(12):1857-67.

56. Ryu S, Shin J-S, Cho Y-W, Kim HK, Paik SH, Lee JH, et al. Fimasartan, anti-hypertension

drug, suppressed inducible nitric oxide synthase expressions via nuclear factor-kappa B and activator protein-1 inactivation. Biological and Pharmaceutical Bulletin. 2013;36(3):467-74

국문초록

서론: NLRP3 인플라마좀 (Inflammasome)은 염증과 세포 사멸에 관여하는 단백질 복합 체로서 caspase I 을 활성화시키고, IL-1ß 분비와 연관된다. 인플라마좀은 염증과 관련된 뇌출혈에서의 중요한 역할로 알려져 있습니다. 피마살탄은 엔지오텐신 II 수용체 차단제로서 고혈압 치료제로 알려져 있고, 심혈관 보호 기능이 보고된 바 있다. 본 연구의 목적은 백서 뇌출혈 모델에서 저 농도 피마살탄, 안지오텐신 수용체 차단제의 하나의, 전 처치 후 NLRP3 인플라마좀 활성화 억제를 통한 뇌 손상 보호 효과에 연구하고자 한다.

방법: 백서 뇌출혈 모델 유발 한달 전부터 피마살탄을 투입하고 또 뇌출혈 2일 후 피마살탄을 투입하여 그 효과를 분석하였다. 피마살탄 저 농도 (0.5 mg/kg)와 상용량 (1.0 mg/kg, 3.0 mg/kg)을 경구로 투약하여 4주 동안 비침습적 방법을 통해 혈압을 측정함. 혈종의 부피, 부종과 뇌출혈 유도된 백서의 기능학적 회복 추적 관찰함. 피마살탄 항염증 작용을 확인하기 위해서, 인플라마좀에(NLRP3, Caspase-1 and IL-1ß) 대한 항체를 이용하여 뇌출혈 주변으로 염증세포가 동원된 정도를 확인하였으며, 특히 저 농도의 피마살탄의 뇌출혈에 대한 보호 효과를 확인하기 위해서 피마살탄은 뇌출혈의 인플라마좀을 western blotting, ELISA, RT-PCR and double immunofluorescent staining 통하여 항염증 관련 세포 신호전달 측정함.

In vitro 시스템에서 성상교세포를 용혈물로 처리하여 뇌출혈의 in vitro 모델을 만들었다. 염증반응을 유발한 후 피마살탄의 염증 조절 반응을 분석하였다.

결과: 피마살탄의 저 농도와 상용량을 뇌출혈 유도 30일간 전 처치 하였을 때는 대조군에 비해, 피마살탄 군에서는 백서 모델에서 형성된 큰 혈종과 부종이 현저히 감소되었고, 기능학적 회복이

증가함. 이러한 결과를 토대로 저 농도의 피마살탄을 뇌출혈 유도 전처리 실험을 진행함. 대조군에 비해 혈압의 저하가 없었으며 염증반응 NLRP3과 NF-kB 신호전달 억제되는 것을 확인함.

성상교세포에 용혈물을 처리하여 뇌출혈 모델을 만들어 실험한 결과 피마살탄은 염증반응을 현저히 완화하였다. 뿐만 아니라 본 연구결과에 의하면 피마살탄은 용혈물에 의한 성상교세포 내의 항염증 반응 효과를 보이며 이는 뇌출혈에 의한 염증 반응 조절 가능성을 보였다.

결론: 피마살탄은 뇌출혈 유도 장기간 전 처리를 한 경우 뇌 손상을 감소시켜 백서의 뇌출혈 모델에서 확인함. 이러한 보호 효과는 항염증 작용에 의해 발생함을 성상교세포를 통한 in vitro 실험과 뇌조직의 형관 염색과 단백질 측정을 통해 확인함. 특히 저 농도의 피마살탄 투약하였을 때 정상 혈압 백서에서 보호 효과를 가질 수 있음을 확인함.

주요어: 안지오텐신 수용체차단제, 피마살탄, 뇌출혈, NLRP3 인플라마좀, 성상교세포, 용혈물,

학번: 2014-31395